SCIENTIFIC REPORTS

OPEN

SUBJECT AREAS:
NANOPHOTONICS AND PLASMONICS
IMAGING AND SENSING

Received
19 June 2014

Accepted
24 September 2014

Published
16 October 2014

Correspondence and requests for materials should be addressed to P.B.C. (pcatryss@stanford.edu)

Complete power concentration into a single waveguide in large-scale waveguide array lenses

Peter B. Catrysse, Victor Liu & Shanhui Fan

Edward L. Ginzton Laboratory and Department of Electrical Engineering, Stanford University, Stanford, CA 94305-4088.

Waveguide array lenses are waveguide arrays that focus light incident on all waveguides at the input side into a small number of waveguides at the output side. Ideal waveguide array lenses provide complete (100%) power concentration of incident light into a single waveguide. While of great interest for several applications, ideal waveguide array lenses have not been demonstrated for practical arrays with large numbers of waveguides. The only waveguide arrays that have sufficient degrees of freedom to allow for the design of an ideal waveguide array lens are those where both the propagation constants of the individual waveguides and the coupling constants between the waveguides vary as a function of space. Here, we use state-of-the-art numerical methods to demonstrate complete power transfer into a single waveguide for waveguide array lenses with large numbers of waveguides. We verify this capability for more than a thousand waveguides using a spatial coupled mode theory. We hereby extend the state-of-art by more than two orders of magnitude. We also demonstrate for the first time a physical design for an ideal waveguide array lens. The design is based on an aperiodic metallic waveguide array and focuses ~100% of the incident light into a deep-subwavelength focal spot.

Waveguide (WG) arrays have been of great interest in optics for several decades[1]. They were first introduced in the context of integrated optical circuits[2]. The initial applications of WG arrays included switches and beam splitters[3–7], high-power semiconductor lasers[8–10], and lenses[11,12]. In recent years, there has been a renewed interest in WG arrays for various linear and nonlinear optics applications[13,14]. From a fundamental point of view, they have been studied in the context of optical analogues of semi-classical electron dynamics[15–18]. Early studies focused primarily on dielectric WG arrays, but metallic WG arrays have attracted much of the attention recently[19–25]. When compared with dielectric WG arrays, metallic WG arrays have different dispersion characteristics and waveguides can support deep-subwavelength modes, which provide important new opportunities for manipulating light at the nanoscale[26].

WG array lenses are arrays of axially invariant waveguides that propagate light incident on all waveguides at the input side of the device and focus or concentrate it into a small number of waveguides at the output side of the device. One may, for example, construct a WG array lens using a ray-optics approach in analogy with a graded index (GRIN) lens[27]. The focal spot in a WG array lens constructed in this manner is confined to quite a few waveguides. In contrast to these conventional WG array lenses, we define here an *ideal* WG array lens as a waveguide array that provides complete power concentration of incident light at its input into a single waveguide at the output[12]. Ideal WG array lenses are of great importance in photonic applications ranging from imaging, where they can provide deep-subwavelength resolution[22], to the combining of optical power generated by an array of laser diodes into a single high-power spot[12]. Reference 12 presents a theoretical design of an ideal WG array lens, based on a coupled mode theory (CMT), for a very small number of waveguides. The design of an ideal WG array lens with a large number of waveguides, which is more relevant for practical applications, is a long-standing unsolved problem.

To solve this problem, two challenges have to be overcome. First, it is not at all evident that an ideal WG array lens exists conceptually for a large number of waveguides. The approach in Ref. 12 is analytic and restricted to a very small number of waveguides (≤7). The only WG arrays of arbitrary size that have been solved completely are fully uniform or synchronous systems both in waveguides and coupling[9], systems with uniform waveguides and a parabolic variation in coupling[11], and systems with a periodic variation in propagation constants and with uniform coupling between the waveguides[28]. None of these systems, however, exhibit ideal WG array lens behaviour. Second, a design for a physical WG array lens structure that achieves complete power concentration in a single waveguide has never been demonstrated for any number of waveguides. Indeed, Ref. 12 only described a way to obtain the CMT parameters of an ideal WG array lens design without reducing this design to practice by showing a physical WG array structure.

Here, we report substantial progress on these two fronts. First, we provide a theoretical plausibility argument for complete power transfer into single waveguide for waveguide array systems with any number of waveguides. A key realization here is that the number of degrees of freedom required to achieve an ideal WG array lens is only available in the most general waveguide arrays where both the propagation constants of individual waveguides and the coupling constants between the waveguides vary as a function of space (in the dimensions transverse to propagation). We verify this argument explicitly with spatial CMT for more than one thousand waveguides. Our theoretical result extends the state-of-art in the field by more than two orders of magnitude. Secondly, we note from our CMT computations that the coupling coefficients of ideal WG array lenses are often negative. This turns out to be the case for metallic waveguide arrays (MWGA)[22]. This observation inspires us to optimize a MWGA structure and demonstrate numerically that it behaves as an ideal WG array lens. The optimized MWGA focuses ~100% of a beam, which is incident on twenty-one waveguides at the input, into a single waveguide at the output. Thus, we show for the first time a physical structure design for an ideal WG array lens. Importantly, our ideal MWGA lens focuses all light into a single deep-subwavelength waveguide ($<\lambda/10$), which in itself is an unusual and remarkable capability. The advances reported here on these two separate fronts solve a longstanding problem in the field of WG arrays. They bring within reach the design of novel light focusing devices and optical power concentrating components for a whole range of exciting photonic applications.

Results

Complete power transfer into a single waveguide: necessary conditions for ideal WG array lenses. Using a spatial CMT, we describe WG arrays in terms of propagation constants (one for each waveguide) and coupling coefficients (between the waveguides). We consider a system with an odd number (N) of waveguides, which are uniform in the axial direction (z) and distributed symmetrically about a centre waveguide (Fig. 1). Further, assume coupling between pairs of nearest neighbour waveguides only, which is reasonable for weakly coupled waveguides. The coupled mode equations for a system with N waveguides are

$$\frac{da_n}{dz} = -j\delta_n a_n - j\kappa_n a_{n+1} - j\kappa_{n-1} a_{n-1} \quad (1)$$

where a_n is the amplitude of the field in guide n with $1 \le n \le N$. The δ_n represent the propagation constant of each waveguide. An overall shift of all the propagation constants by the same amount does not change the dynamics of the intensities in the waveguides, therefore the δ_n's are the shifted propagation constants where the overall shift is chosen to facilitate numerical treatment. The δ_n's are symmetrically distributed about the centre waveguide $n = (N + 1)/2$. The coupling between waveguides is given by the coupling coefficients κ_n, where $\kappa_0 = \kappa_N = 0$ for the outside waveguides $n = 1$ and $n = N$. Power conservation and reciprocity require $(d/dz)\Sigma_n|a_n|^2 = 0$ and real κ_n's in lossless systems. For $\exp(-j\beta z)$ dependence, the system eigenvalues β_n (propagation constants) are real and the characteristic modes of the system are given by the eigenvectors v_n.

We assume an initial excitation with uniform amplitude and identical phase for all the waveguides. This excitation is symmetric with respect to the centre waveguide and only the $(N + 1)/2$ symmetric eigenvectors are of interest. We define an equivalent "reduced" waveguide array system with $(N + 1)/2$ eigenvalues. The reduced $(N + 1)/2$ -waveguide system has the same eigenvalues β_n and, therefore, the same δ_n and κ_n as the original system for $1 \le n \le (N - 1)/2$. Only

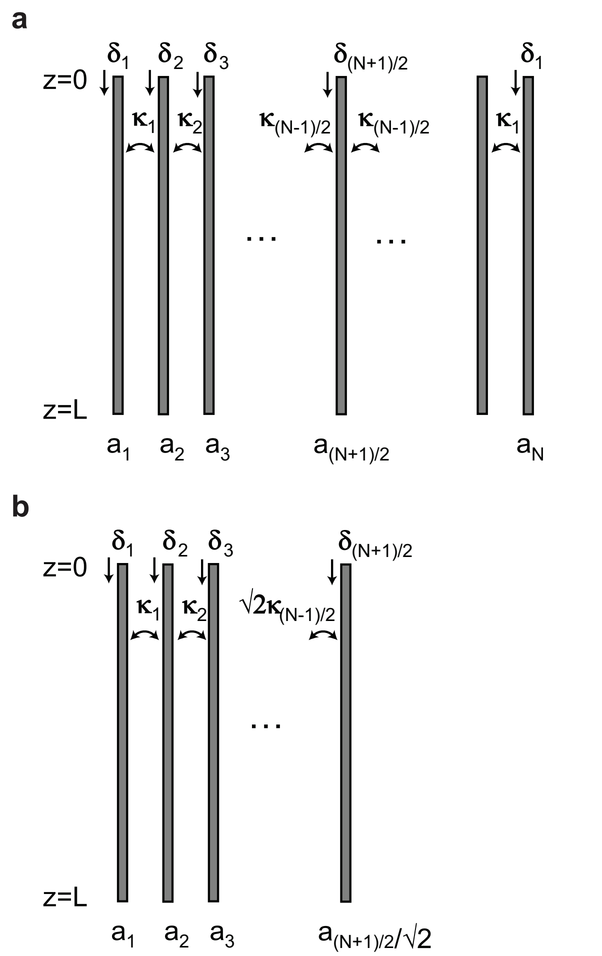

Figure 1 | Waveguide (WG) array with an odd number (N) of waveguides that are uniform in the axial (z) direction and distributed symmetrically about a centre waveguide. (a) Spatial coupled mode theory (CMT) description of WG array in terms of each waveguide's propagation constant δ_n and the coupling coefficient κ_n between adjacent waveguides with $1 \le n \le N$. The input of the WG array is at $z = 0$ and the output at $z = L$. The a_n are the amplitudes of the fields in guide n. (b) Equivalent "reduced" CMT description of the WG array making use of symmetry about the centre waveguide.

the coupling coefficient of the centre waveguide of the original N-th order system $\kappa_{(N-1)/2}$ differs[12]. The reduced waveguide system has $(N + 1)/2$ δ's and $(N - 1)/2$ κ's. These can be adjusted independently, which results in $(N + 1)/2 + (N - 1)/2 = N$ degrees of freedom.

By imposing boundary conditions at the output, we now demonstrate that this system has the necessary number of degrees of freedom to provide complete power concentration in a single waveguide. We consider the general case where the complex input amplitudes in all waveguides are specified. The desired system response at the output consists of zero amplitude in all waveguides except for one in which all light is concentrated at focus. This yields a set of $(N + 1)/2$ complex equations. Shifting the phase of the light in the single waveguide at focus does not affect the output intensity. The set is thus reduced to N real system constraints. Since there are also N real adjustable parameters, the system constraints can in principle be satisfied. This proves that WG arrays with $(N + 1)/2$ δ's and $(N - 1)/2$ κ's have the necessary number of adjustable parameters to design an ideal WG array lens that focuses all light into a single waveguide.

The theoretical plausibility argument we provide here is very general, and points to the possible existence of an ideal WG array lens with any number of waveguides. This argument, however, does not

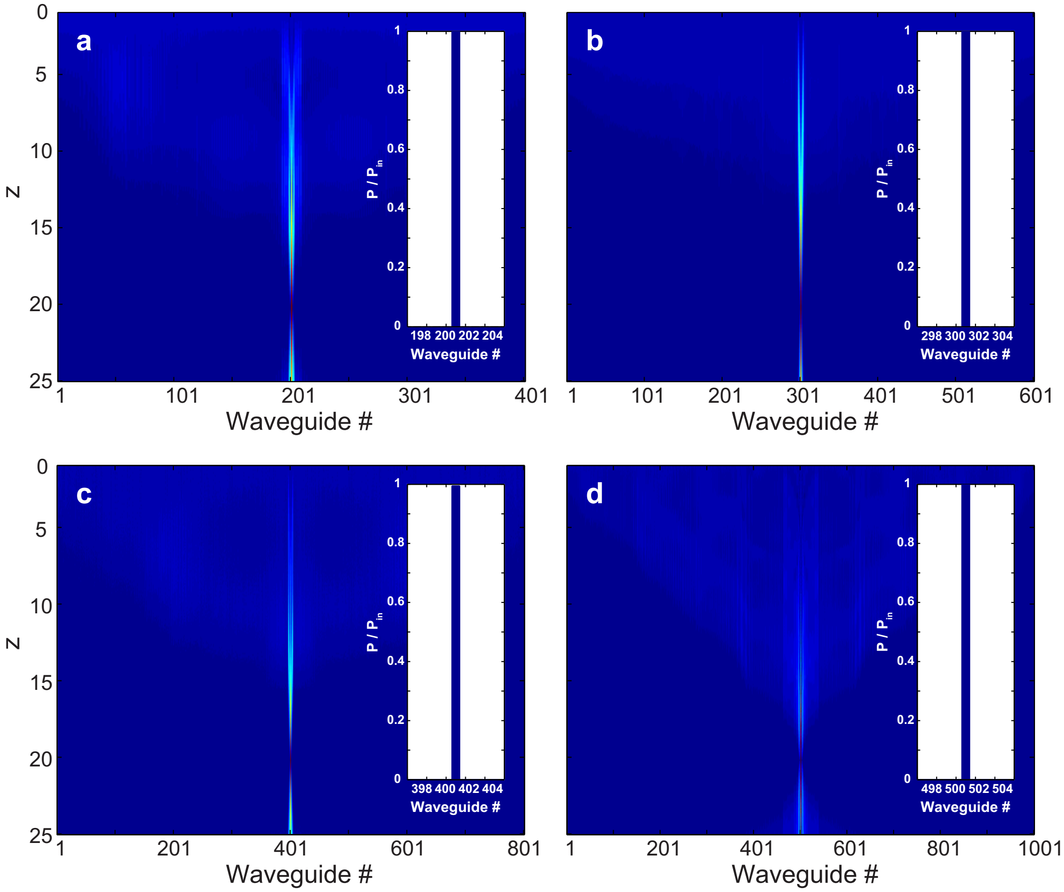

Figure 2 | Ideal WG array lens designs with up to more than one thousand waveguides optimized for single waveguide focusing. The power distribution at the input of the guides ($z = 0$) is uniform. Bar plots show power versus waveguide number in the WG array lens at the focal length ($z = L = 20$) for $N = 401$ (a), $N = 601$ (b), $N = 801$ (c), and $N = 1001$ (d). Results are obtained starting from a random set of initial values for coupling coefficients κ_n and shifted propagation constants δ_n.

provide us with an ideal WG array lens design. Reference 12 shows that designs exist for $N \leq 7$ with an approach that requires full analytical expressions for the eigenvalues β_n and eigenvectors v_n (in terms of δ_n and κ_n). This approach can not be generalized for $N > 7$.

Complete power transfer into a single waveguide for large-scale WG array lenses: a numerical optimization based on spatial CMT. Instead of requiring a full analytical treatment of the eigensystem solutions, which limits the size of the problem that can be solved, we combine spatial CMT with efficient numerical eigensystem solvers and optimization methods that run on high performance computational hardware. This allows us to specify and optimize the parameters for very large WG array lenses. We use local optimization schemes in this work, but our approach is very general and can easily be extended to take advantage of modern global optimization methods. This way, in principle, we can design ideal WG array lenses with any number of waveguides. The optimization of a design involves computing the eigenvalues of a system matrix a large number of times before convergence is achieved. Thus, the use of efficient numerical eigensystem solvers is essential to complete the optimization process. In this work, we use an implementation of the algorithm of multiple relatively robust representations (MRRR), which computes orthogonal eigenvectors of a symmetric tridiagonal system matrix with $O(n^2)$ cost[29].

Figure 2 shows numerical results for ideal WG array lens designs up to more than one thousand waveguides optimized for focusing into a single centre waveguide at the focal length. In these CMT calculations, we assume an initial condition with a uniform phase distribution, corresponding to normal incidence for a physical WG array lens. The insets show bar plots of the power in the centre waveguides, as a function of waveguide number, at focus for $N = 401$ (a), $N = 601$ (b), $N = 801$ (c), and $N = 1001$ (d). In all cases, 100% of the power is concentrated in the centre waveguide at the focus of the WG array lens design. These results confirm, for the first time, that it is possible to design an ideal WG array lens with a very large number of waveguides. We note that these designs are scale invariant. In our calculations, we chose a focal length $L = 20$ and that determined the range of (dimensionless) κ_n and δ_n values. To convert this design into physical units, one can convert this focal length into an absolute distance with a scalar scaling factor and that in turn dictates the scaling of κ_n and δ_n as well. We also note that each design is obtained by starting from a random set of initial values for κ_n and δ_n. This demonstrates the robustness of our (local) optimization approach for designing ideal WG array lenses.

We now consider the angular response of ideal WG array lenses. For oblique incidence, we apply a linear phase tilt in the initial condition in the CMT formalism. Next, we will analyze an ideal WG array lens with $N = 801$ waveguides, which has been optimized to focus into a single waveguide under uniform phase illumination. Figure 3 shows the response of the ideal WG array lens when the incident illumination has a linear phase tilt quantified by the total phase shift across the device. A bar plot insets show the power in the centre waveguides as a function of waveguide number at the focal length of the ideal WG array lens. Figure 3a reviews uniform phase illumination (normal incidence). The ideal WG array lens is optimized for this normal incidence and focuses 100% of the incident

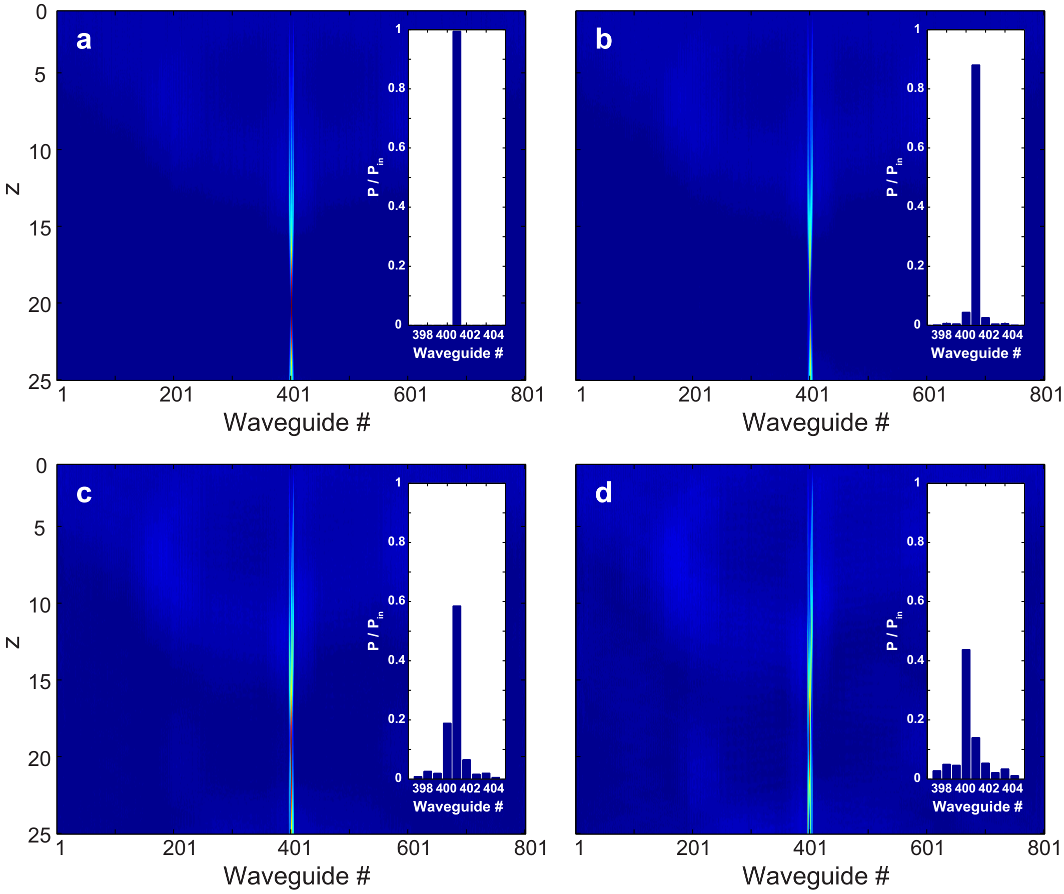

Figure 3 | Angular response of an ideal WG array lens design with $N = 801$ waveguides optimized for single waveguide focusing. The power distribution at the input of the guides ($z = 0$) is uniform. Bar plots show power versus waveguide number in the WG array lens at the focal length ($z = L = 20$) for (a) normal incidence (optimized for this type of illumination) and for oblique incidence with a phase shift across the array of (b) 1.20 rad, (c) 2.46 rad, and (d) 4.36 rad. Results are obtained starting from the same random set of initial values for coupling coefficients κ_n and shifted propagation constants δ_n as for the design shown in Fig. 2c.

light in a single waveguide. Figure 3b shows the response for oblique incidence illumination with a 1.20 radians phase shift across the array. The WG array lens still focuses ~90% of the optical power into a single waveguide. As the phase shift is increased to 2.46 radians in Fig. 3c, the focal spot shifts further away from the centre waveguide and is contained in two adjacent waveguides. For larger phase shifts (e.g., 4.36 radians in Fig. 3d), the focal spot remains very well defined and shifts to the next waveguide. Note that these phase shifts can be converted into oblique illumination angles when the CMT is applied to a physical structure. This analysis demonstrates that an ideal WG array lens design exhibits excellent focusing even when a tilted wavefront is present at the input. The result is near 100% concentration in a single waveguide. This ideal behaviour persists for a wide range of phase shifts. The angular response of the focusing behaviour in ideal WG array lenses is therefore reminiscent of the optical "memory effect"[30,31] and the role it plays in focusing or even imaging through disordered media by means of wavefront-shaping[32]. The memory effect refers to the fact that phase gradients are partially conserved when light propagates through disordered or random media. When a wavefront shape is engineered to achieve a focal spot at a certain location following propagation through random media, it has been shown that a small tilt of the same wavefront also results in a focal spot, albeit it in a location shifted from the original spot[32].

We now illustrate that the design of an ideal WG array lens deviates significantly in its parameter values from an intuitive design, such as that based on a GRIN lens design where a quadratic index profile is known to produce focusing[33,34].

First, we derive the CMT parameters of a GRIN WG array lens. One may design a GRIN WG array lens by obtaining Eq. (1) as a discretized version of the paraxial wave equation for a medium with gradient index $n(x)$. To produce focusing, we consider a medium with a half-width h and a quadratic index profile ranging from n_0 at the centre to 1 at the edge,

$$n(x) = n_0\left(1 - \frac{n_0 - 1}{n_0}\frac{x^2}{h^2}\right) \tag{2}$$

We can write the paraxial wave equation in this inhomogeneous medium as

$$2jk\frac{\partial\psi}{\partial z} = \nabla_\perp^2\psi - V(x)\psi \tag{3}$$

where $k(x) = k_0\, n(x) = \frac{2\pi}{\lambda} n(x)$. $V(x)$ is a quadratic potential due to the index gradient,

$$V(x) \approx 2k_0^2 n_0^2 \frac{n_0 - 1}{n_0}\frac{x^2}{h^2} \tag{4}$$

We discretize Eq. (3) using central differences with a step size Δ

$$2jk_0 n_0\frac{\partial\psi(x_n)}{\partial z} = -\left[\frac{2}{\Delta^2} + V(x_n)\right]\psi(x_n) + \frac{1}{\Delta^2}\psi(x_n + \Delta) + \frac{1}{\Delta^2}\psi(x_n - \Delta) \tag{5}$$

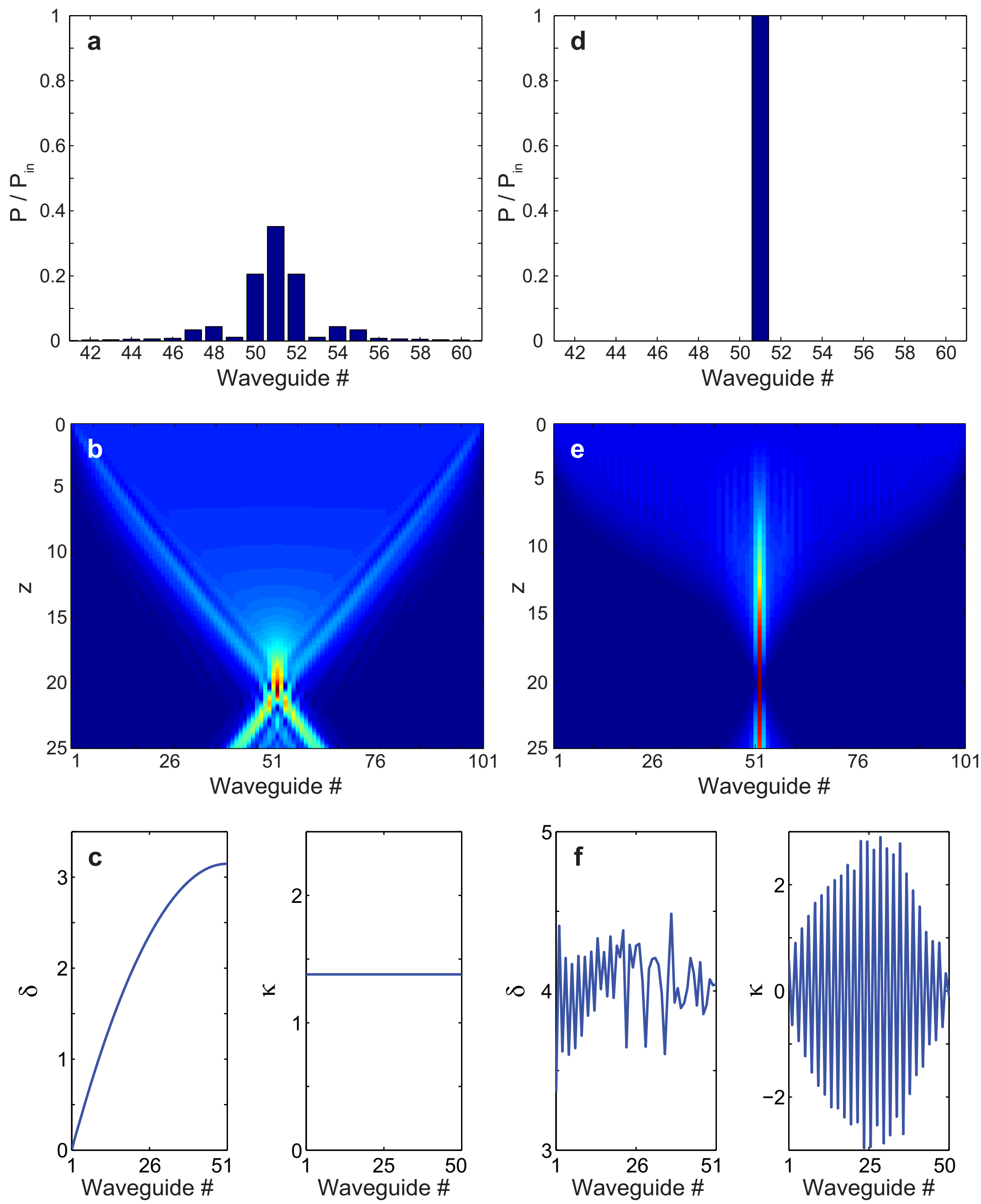

Figure 4 | Focusing in WG array lenses. The WG array lens designs comprise $N = 101$ waveguides and the power distribution at the input of the guides ($z = 0$) is uniform. (a,b) Graded index (GRIN) WG array lens design in which the focal spot at $z = L = 20$ consists of the excitation of quite a few waveguides at the centre of the array. (c) The parameter values for the GRIN WG array lens in (a,b) with a quadratic dependence of δ_n versus waveguide number and constant κ_n. (d,e) Ideal WG array lens design which provides complete power concentration of light incident on its waveguides at the input into a single waveguide at the output ($z = L = 20$). (f) The parameter values for an ideal WG array lens with optimized δ_n and κ_n.

and compare the result with the coupled mode equations Eq. (1). This allows us to identify the CMT parameters

$$\delta(x_n) = -\frac{1}{k_0 n_0 \Delta^2} - k_0 n_0 \frac{n_0 - 1}{n_0}\frac{x_n^2}{h^2}, \quad \kappa = \frac{1}{2k_0 n_0 \Delta^2} \qquad (6)$$

of a GRIN waveguide array lens with quadratic index profile Eq. (2).

Figure 4 shows the focusing behaviour of a conventional GRIN WG array lens (a,b) and the single-waveguide focus in an ideal WG array lens (d,e) with $N = 101$ waveguides. The GRIN WG array lens design results in good focusing, but only $<$40% of the light is contained within the centre waveguide. The ideal WG array lens, by contrast, focuses 100% of the power that is incident on the lens into the centre waveguide at the focal plane. Figure 4c,f contrasts the parameter values for κ_n and δ_n for the respective WG array lenses. Figure 4c represents the conventional GRIN WG array lens parameters with a quadratic dependence of δ_n and constant κ_n. Figure 4f shows the optimized parameter values for an ideal WG array lens obtained via a numerical parameter optimization. The parameters for the ideal WG array lens in Fig. 4f deviate significantly from those of the GRIN WG array lens design in Fig. 4c. These results illustrate explicitly that an ideal WG array lens requires highly counter-intuitive design parameters, i.e., parameters that deviate significantly from those of more intuitive designs, such as a quadratically varying index profile that leads to focusing in continuous GRIN lenses and discrete GRIN WG array lenses.

We observe that the coupling coefficients for an ideal WG array lens design have both negative and positive signs (Fig. 4f), in contrast to the more intuitive GRIN WG array lens where the coupling constant is positive. It turns out that negative coupling between adjacent waveguides occurs naturally in a MWGA[22]. MWGAs are also quite interesting due to their unusual capabilities for deep sub-wavelength light manipulation. This motivates the design of physical structures using MWGAs. We note that negative coupling, in general, can be achieved when the fundamental waveguide mode is odd[35]. Incidentally, this is also possible in all-dielectric arrays based on photonic crystal waveguides[36].

Near-complete power transfer into single waveguide for a physical structure based on MWGAs. In this section, we demonstrate that ideal WG array lenses can be realized in MWGA structures (Fig. 5a). The choice of MWGAs is motivated in part by the CMT study above, which observes that an ideal WG array lens tends to have negative coupling constants. While waveguide arrays have been studied before, none of the physical designs, including MWGA designs previously published, has been shown to focus *all* of the incident power into a single waveguide.

Figure 5 shows an ideal WG array lens design based on a MWGA structure using a lossless metal. The MWGA geometry using lossless gold (yellow regions) and air (blue regions) is shown in Fig. 5a. The parameters of the structure design, i.e., the widths of the waveguides (air) and their separations (gold), are optimized using a semi-analytic beam propagation method based on finite-differences so that the lens achieves focusing of *all* incident light into a single waveguide. Figure 5b,c show the cross-sectional plot of magnetic field magnitude squared versus distance and at the focal plane (focal length $L = 19.5\ \mu m$), respectively. The structure focuses 100% the power incident optical power into the centre waveguide and thus acts as an ideal MWGA lens with $N = 21$ waveguides ($\lambda = 1\ \mu m$).

Figure 6 shows an ideal WG array lens structure based on a MWGA using realistic metal properties. A semi-analytic beam propagation method is used to optimize the MWGA lens design at $\lambda = 1\ \mu m$ with measured optical properties for gold[37]. Figure 6a shows a cross-sectional plot of the squared magnitude of the magnetic field versus distance inside an ideal MWGA lens design ($N = 21$). Figure 6b shows the squared magnitude of the magnetic field versus transverse spatial coordinates at focus ($L = 19.5\ \mu m$). Despite material loss, the MWGA structure focuses 99% of the power at the focal plane into the centre waveguide. It clearly demonstrates that an ideal WG array lens can be designed using realistic (lossy) metals.

These ideal MWGA lenses demonstrate for the first time that it is possible to design a structure that focuses 100% of the incident power into the centre waveguide at the focal length (lossless MWGA structure) and that a properly designed lossy MWGA structure can collect nearly 100% of the light into a single waveguide.

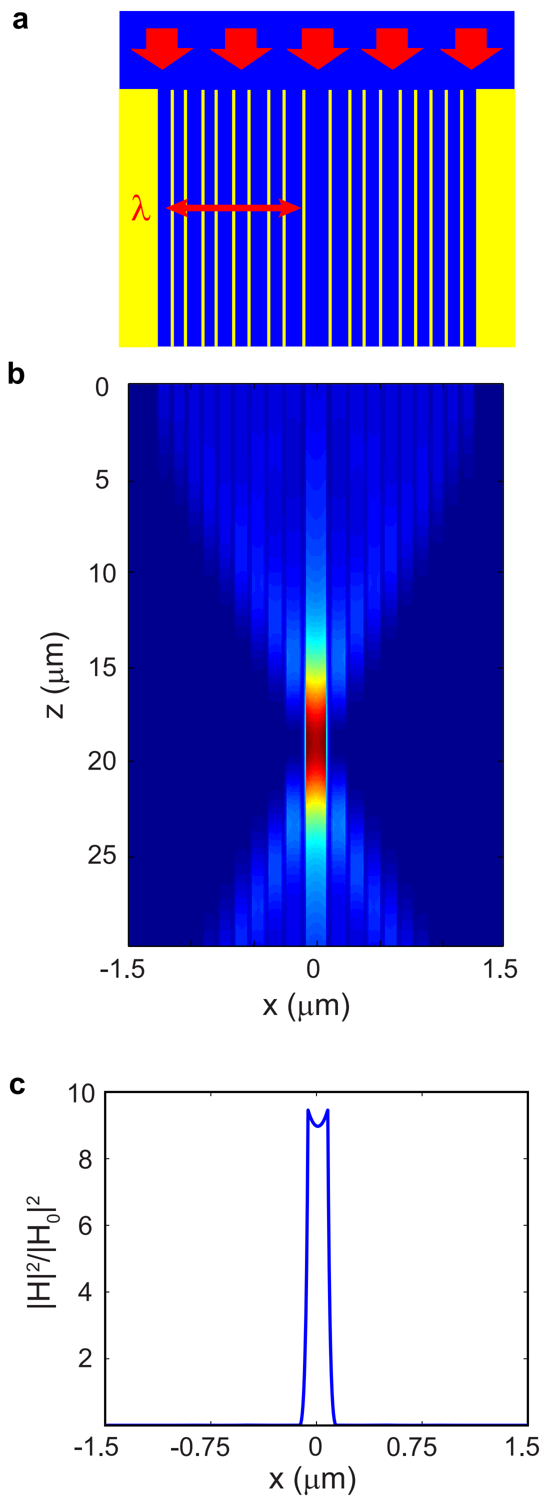

Figure 5 | Ideal WG array lens structure based on a metallic waveguide array (MWGA) using lossless metal. (a) MWGA structure geometry using gold (yellow regions) and air (blue regions). (b,c) Cross-sectional plot of field magnitude squared versus distance and at focus (focal length $L = 19.5\ \mu m$) for an ideal MWGA lens with $N = 21$ waveguides ($\lambda = 1\ \mu m$). This lossless design was optimized using a semi-analytic beam propagation method based on finite-differences.

Discussion

We used spatial CMT and state-of-the-art numerical methods to demonstrate the design of ideal WG array lenses with a very large number of waveguides. Our results suggest that complete power transfer into single waveguide is achievable for WG arrays of any size. We verified this behaviour explicitly up to more than a thousand waveguides, thereby extending the state-of-art in the field by several orders of magnitude.

The ideal WG array lens designs have parameter values that differ significantly from those that one might obtain using physical intuition derived from a GRIN lens based approach. They are obtained through our systematic design approach based on spatial CMT, numerical optimization with fast eigensystem solvers, and semi-analytic beam propagation. Notably, the CMT coupling parameters observed in ideal WG array lens designs are often negative, which motivated us to demonstrate this capability in MWGA geometry. We designed and numerically demonstrated ideal WG array lens behaviour for the first time in a physically realizable MWGA structure. Moreover, MWGAs have been shown to enable deep-subwavelength

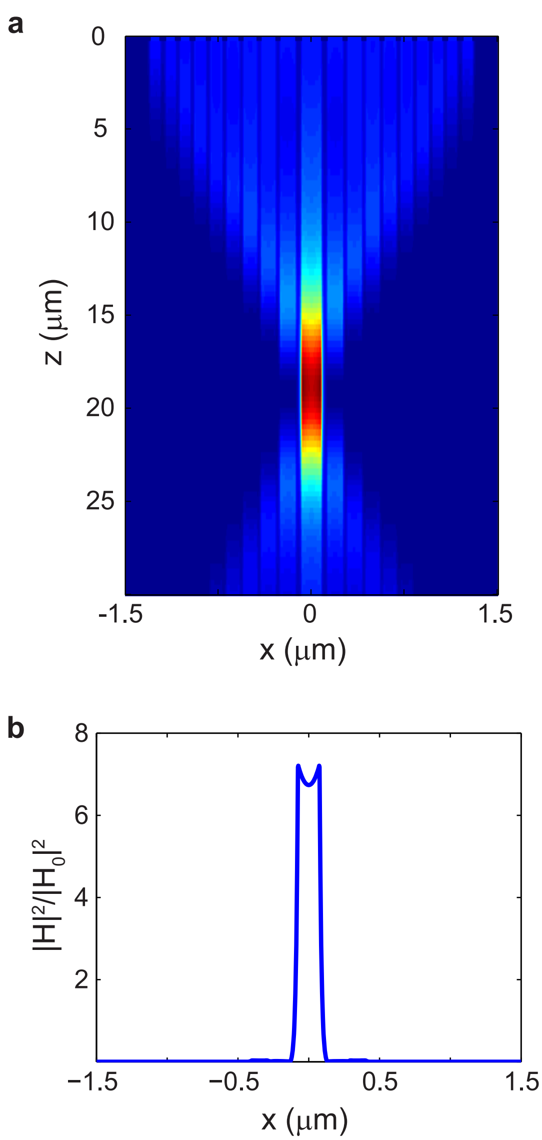

Figure 6 | Ideal WG array lens structure based on a MWGA using realistic metal properties. A semi-analytic beam propagation method is used to optimize the MWGA lens structure ($N = 21$) with measured optical properties for gold at $\lambda = 1\ \mu m$. (a) Cross-sectional plot of field magnitude squared versus distance inside the ideal MWGA lens structure. (b) Field magnitude squared versus transverse spatial coordinates at focus ($L = 19.5\ \mu m$).

focusing over a long focal distance, which is of substantial interest in nanophotonics[22]. We have now shown that *all* the power can be focused into a single waveguide that is deep-subwavelength ($<\lambda/10$) in a structure that has a simple planar geometry. This makes our practical realization even more remarkable.

The spatial CMT approach used in this work is very general. It does not imply or restrict the design to a specific structure, geometry or material system. The results can therefore apply to any WG array system where nearest neighbour coupling dominates. The theoretical results presented here are thus relevant for dielectric WG arrays, e.g., with conventional low index contrast waveguides or integrated high index contrast waveguides, as well as for MWGAs.

In summary, our methodology applied on two separate fronts solves a longstanding problem in the field. Moreover, it propels WG array lens design forward, bringing within reach a whole range of very exciting applications, including deep-subwavelength imaging and high-power solid-state laser arrays.

Methods

Spatial coupled mode theory (CMT). Our approach for specifying the parameters for any order waveguide array lens is based on spatial CMT. In the numerical CMT method, we use optimization, rather than finding analytical expressions for the eigenvalues and eigenvectors in terms of the propagation constants δ_n and the coupling coefficients κ_n, followed by applying the input/output boundary conditions to determine κ_n and δ_n. Based on Eq. (1), we derive the full system matrix assuming nearest neighbour coupling

$$A = -j\begin{pmatrix} \delta_1 & \kappa_1 & & & & & & & \\ \kappa_1 & \delta_2 & \kappa_2 & & & & & & \\ & & \ddots & & & & & & \\ & & & \ddots & & & & & \\ & & & \kappa_{\frac{(N-1)}{2}} & \delta_{\frac{(N-1)}{2}} & \kappa_{\frac{(N-1)}{2}} & & & \\ & & & & & \ddots & & & \\ & & & & & & \ddots & & \\ & & & & & & \kappa_2 & \delta_2 & \kappa_1 \\ & & & & & & & \kappa_1 & \delta_1 \end{pmatrix} \quad (7)$$

and the equivalent "reduced" system matrix

$$A' = -j\begin{pmatrix} \delta_1 & \kappa_1 & & \\ \kappa_1 & \delta_2 & \kappa_2 & \\ & & \ddots & \\ & & & \ddots \\ & & \sqrt{2}\kappa_{(N-1)/2} & \delta_{(N+1)/2} \end{pmatrix} \quad (8)$$

with appropriately scaled input amplitude and output amplitude for the centre $(N + 1)/2$ waveguide. The general solution of Eqs. (7–8) has the form

$$a_m(z) = \sum_{n=1}^{N} A_n v_n(m) e^{-j\beta_n z} \quad (9)$$

where β_n is the nth eigenvalue of the system matrix, v_n is the corresponding eigenvector, and A_n is the coefficient determined by the boundary conditions. We start with a given set of initial values for the κ_n and δ_n, and we calculate numerically how well the field amplitudes a_m at the output satisfies the output boundary condition following a uniform field excitation at the input. We then optimize this initial design until it provides the required output field amplitudes with all light in the centre waveguide and no light (zero amplitudes) in the remaining waveguides. Unlike the analytical approach, which is limited to a small number of waveguides $N \leq 7$, this numerical method allows us to design WG array lenses with hundreds and even thousands of waveguides. To achieve this, it requires the efficient computation of the full set of eigenvalues of the system matrix Eqs. (7–8).

Semi-analytic beam propagation method based on finite-differences. We are interested in transverse-magnetically (TM) polarized propagation in longitudinally (z) invariant waveguiding structures. The dielectric constant is assumed to be piecewise constant in the transverse direction (x). Starting with Maxwell's equations, we consider the propagation direction to be z, and the transverse direction is x. For TM polarization, there is only H_y and E_x and E_z. Hence, the expressions reduce in terms of H_y to

$$\frac{\partial^2}{\partial z^2} H_y = -\left(\omega^2 \mu\varepsilon + \varepsilon \frac{\partial}{\partial x}\frac{1}{\varepsilon}\frac{\partial}{\partial x}\right) H_y \quad (10)$$

We discretize the propagation equation using finite differences. Choosing N interior nodes (so there are N + 1 intervals, assuming the endpoint nodes are fixed to zero). Collecting all equations, this immediately leads to a system of coupled ordinary differential equations:

$$\frac{\partial^2}{\partial z^2} H = -AH \quad (11)$$

where A is tridiagonal with positive diagonal elements when $\varepsilon > 0$. Note that this discretization does not result in symmetric matrices. In order to obtain a symmetric system, we must form

$$\frac{1}{\varepsilon}\frac{\partial^2}{\partial z^2} H = -\frac{1}{\varepsilon} AH \quad (12)$$

The solution to the propagation equation requires solving the eigenvalue problem to determine the full modal decomposition in the x direction. We obtain a matrix system

$$Kv = \beta^2 Mv \quad (13)$$

where K and M are both symmetric tridiagonal matrices (note that M is not necessarily positive definite, although it is almost always non-singular, and possibly complex). If the system is assumed to possess mirror symmetry in the x direction, then the matrices are also persymmetric.

Numerical eigensystem solvers. The numerical eigenvalue problems that arise in the spatial CMT approach and the finite-difference simulations of physical structures lead to tridiagonal system matrices. The conventional widely-used state-of-the-art method is the QR or QZ iteration, which does not preserve the tridiagonal structure. The expected runtime of this approach is therefore $O(N^3)$. Here, we use the algorithm of multiple relatively robust representations (MRRR) that computes orthogonal eigenvectors of a symmetric tridiagonal system matrix A (or A′) with $O(N^2)$ cost[29]. There exists also an experimental method based on the Ehrlich-Aberth iteration with an expected runtime of approximately $O(N^2)$[38]. Preliminary experiments have been very promising for this method, however generalizations of the method to the fully tridiagonal system have encountered non-converging cases.

1. Syms, R. R. A. Perturbation analysis of nearly uniform coupled wave-guide arrays. *Appl. Opt.* **25**, 2988–2995 (1986).
2. Yariv, A. Coupled-mode theory for guided-wave optics. *IEEE J. Quantum Electron.* **QE-9**, 919–933 (1973).
3. Alferness, R. C. Waveguide electrooptic modulators. *IEEE Trans. Microwave Theory Tech.* **30**, 1121–1137 (1982).
4. Elachi, C. & Yeh, C. Distribution networks and electrically controllable couplers for integrated optics. *Appl. Opt.* **13**, 1372–1375 (1974).
5. Haus, H. A. & Fonstad, C. G. Three-waveguide couplers for improved sampling and filtering. *IEEE J. Quantum Electron.* **QE-17**, 2321–2325 (1981).
6. Marcatili, E. A. J. Dielectric rectangular waveguide and directional coupler for integrated optics. *Bell Syst. Tech. J.* **48**, 2071–2102 (1969).
7. Papuchon, M. *et al.* Electrically switched optical directional coupler - Cobra. *Appl. Phys. Lett.* **27**, 289–291 (1975).
8. Ackley, D. E. Single longitudinal mode-operation of high-power multiple-stripe injection-lasers. *Appl. Phys. Lett.* **42**, 152–154 (1983).
9. Butler, J. K., Ackley, D. E. & Botez, D. Coupled-mode analysis of phase-locked injection-laser arrays. *Appl. Phys. Lett.* **44**, 293–295 (1984).
10. Ripper, J. E. & Paoli, T. L. Optical coupling of adjacent stripe-geometry junction lasers. *Appl. Phys. Lett.* **17**, 371–373 (1970).
11. Haus, H. A. & Molter-Orr, L. Coupled multiple waveguide systems. *IEEE J. Quantum Electron.* **19**, 840–844 (1983).
12. Haus, H. A., Molter-Orr, L. & Leonberger, F. J. Multiple waveguide lens. *Appl. Phys. Lett.* **45**, 19–21 (1984).
13. Christodoulides, D. N. & Joseph, R. I. Discrete self-focusing in nonlinear arrays of coupled wave-guides. *Opt. Lett.* **13**, 794–796 (1988).
14. Christodoulides, D. N., Lederer, F. & Silberberg, Y. Discretizing light behaviour in linear and nonlinear waveguide lattices. *Nature* **424**, 817–823 (2003).
15. Khomeriki, R. & Ruffo, S. Nonadiabatic Landau-Zener tunneling in waveguide arrays with a step in the refractive index. *Phys. Rev. Lett.* **94**, 113904 (2005).
16. Lenz, G., Talanina, I. & de Sterke, C. M. Bloch oscillations in an array of curved optical waveguides. *Phys. Rev. Lett.* **83**, 963–966 (1999).
17. Morandotti, R., Peschel, U., Aitchison, J. S., Eisenberg, H. S. & Silberberg, K. Experimental observation of linear and nonlinear optical Bloch oscillations. *Phys. Rev. Lett.* **83**, 4756–4759 (1999).
18. Peschel, U., Pertsch, T. & Lederer, F. Optical Bloch oscillations in waveguide arrays. *Opt. Lett.* **23**, 1701–1703 (1998).
19. Fan, X. B. & Wang, G. P. Nanoscale metal waveguide arrays as plasmon lenses. *Opt. Lett.* **31**, 1322–1324 (2006).
20. Fan, X. B., Wang, G. P., Lee, J. C. W. & Chan, C. T. All-angle broadband negative refraction of metal waveguide arrays in the visible range: Theoretical analysis and numerical demonstration. *Phys. Rev. Lett.* **97**, 073901 (2006).
21. Conforti, M., Guasoni, M. & De Angelis, C. Subwavelength diffraction management. *Opt. Lett.* **33**, 2662–2664 (2008).
22. Verslegers, L., Catrysse, P. B., Yu, Z. F. & Fan, S. H. Deep-subwavelength focusing and steering of light in an aperiodic metallic waveguide array. *Phys. Rev. Lett.* **103**, 033902 (2009).
23. Davoyan, A. R., Shadrivov, I. V., Sukhorukov, A. A. & Kivshar, Y. S. Plasmonic Bloch oscillations in chirped metal-dielectric structures. *Appl. Phys. Lett.* **94**, 161105 (2009).
24. Bartal, G., Lerosey, G. & Zhang, X. Subwavelength dynamic focusing in plasmonic nanostructures using time reversal. *Phys. Rev. B* **79**, 201103 (2009).
25. Grajower, M. *et al.* Subwavelength plasmonics for graded-index optics on a chip. *Opt. Lett.* **38**, 3492–3495 (2013).
26. Economou, E. N. Surface plasmons in thin films. *Phys. Rev.* **182**, 539–554 (1969).
27. Kawakami, S. & Haus, H. A. Continuum analog of coupled multiple wave-guides. *J. Lightwave Technol.* **4**, 160–168 (1986).
28. Syms, R. R. A. Characteristic mode theory of coupled wave-guide arrays with periodically varying properties. *Appl. Opt.* **25**, 724–731 (1986).
29. Dhillon, I. S. & Parlett, B. N. Multiple representations to compute orthogonal eigenvectors of symmetric tridiagonal matrices. *Linear Algebra Appl.* **387**, 1–28 (2004).
30. Feng, S. C., Kane, C., Lee, P. A. & Stone, A. D. Correlations and fluctuations of coherent wave transmission through disordered media. *Phys. Rev. Lett.* **61**, 834–837 (1988).
31. Freund, I., Rosenbluh, M. & Feng, S. Memory effects in propagation of optical waves through disordered media. *Phys. Rev. Lett.* **61**, 2328–2331 (1988).
32. Katz, O., Small, E. & Silberberg, Y. Looking around corners and through thin turbid layers in real time with scattered incoherent light. *Nature Photon.* **6**, 549–553 (2012).
33. Haus, H. A. *Waves and fields in optoelectronics*. (Prentice-Hall, Englewood Cliffs, NJ; 1984).
34. Levy, U. *et al.* Inhomogenous dielectric metamaterials with space-variant polarizability. *Phys. Rev. Lett.* **98**, 243901 (2007).
35. Locatelli, A., Conforti, M., Modotto, D. & De Angelis, C. Diffraction engineering in arrays of photonic crystal waveguides. *Opt. Lett.* **30**, 2894–2896 (2005).
36. de Sterke, C. M., Botten, L. C., Asatryan, A. A., White, T. P. & McPhedran, R. C. Modes of coupled photonic crystal waveguides. *Opt. Lett.* **29**, 1384–1386 (2004).
37. Palik, E. D. & Ghosh, G. *Handbook of optical constants of solids*. (Academic Press, Orlando; 1985).
38. Bini, D. A., Gemignani, L. & Tisseur, F. The Ehrlich-Aberth method for the nonsymmetric tridiagonal eigenvalue problem. *SIAM J. Matrix Anal. Appl.* **27**, 153–175 (2005).

Acknowledgments

This work was supported by a US Air Force STTR Phase II award (Contract FA8650-12-C-1472) in collaboration with Holochip Corporation. We thank R. Batchko, P. Marasco and S. Robinson for fruitful discussions and critical feedback.

Author contributions

P.C. and S.F. initiated and supervised the project. V.L. developed the semi-analytic beam propagation method and implemented several experimental algorithms to compute the eigenvalues of a system matrix. V.L. and P.C. performed the spatial CMT calculations and the eigensystem-based numerical optimization. All authors discussed the results and contributed to the manuscript.

Additional information

Competing financial interests: The authors declare no competing financial interests.

How to cite this article: Catrysse, P.B., Liu, V. & Fan, S. Complete power concentration into a single waveguide in large-scale waveguide array lenses. *Sci. Rep.* **4**, 6635; DOI:10.1038/srep06635 (2014).